ELSEVIER

Computer Methods and Programs in Biomedicine 45 (1994) 175–186

computer methods and programs in biomedicine

A computer simulation study on the input function sampling schedules in tracer kinetic modeling with positron emission tomography (PET)

Dagan Feng*[a], Xinmin Wang[a], Hong Yan[b]

[a]*Basser Department of Computer Sciences, F09, The University of Sydney, Sydney, N.S.W. 2006, Australia*
[b]*Department of Electrical Engineering, The University of Sydney, Sydney, N.S.W. 2006, Australia*

Received 5 August 1993; revision received 1 June 1994; accepted 10 June 1994

Abstract

Tracer kinetic modeling with positron emission tomography (PET) requires measurements of the time-activity curves in both plasma (PTAC) and tissue (TTAC) to estimate physiological parameters, i.e. to fit the parameters of certain compartmental models using PTAC and TTAC as the model input and output functions, respectively. In this paper, we first explored the optimal blood sampling schedule (OBSS) for the input function, based on the tracer [^{18}F]2-fluoro-2-deoxy-D-glucose (FDG) blood sample experimental data. Then using a 5-parameter FDG model we investigated the effects of the plasma sampling schedule, as well as PTAC measurement noise, on the estimation accuracy and reliability of FDG model macro- and micro-parameters and the physiological parameter local cerebral metabolic rates of glucose (LCMRGlc), using computer simulation. Three different methods were used: (a) estimation of the FDG model parameters ignoring PTAC noise using the traditional PTAC schedule (non-OBSS); (b) estimation of the PTAC model parameters and FDG model parameters simultaneously using both non-OBSS and OBSS; (c) estimation of the PTAC model parameters first, then the FDG model parameters using both non-OBSS and OBSS. The results show that OBSS can provide more reliable estimates and largely simplifies the experiment operations.

Keywords: Computer simulation; Modeling; PET; Optimal blood sampling schedule

1. Introduction

Tracer kinetic modeling techniques have been widely used in studying metabolic, pharmacokinetic and other biochemical processes in humans with positron emission tomography (PET) [1]. Application of kinetic modeling techniques can provide improved understanding of the dynamic processes [2]. In general, tracer kinetic modeling requires measurements of the time-activity curves in both plasma (PTAC) and tissue (TTAC) to estimate the physiological parameters, i.e. to fit the parameters of certain compartmental models, (e.g., the 3-compartment [^{18}F]-fluoro-2-deoxy-D-glucose (FDG) model in Fig. 1, using PTAC and

* Corresponding author, Tel.: 61 2 692 2103; Fax: 61 2 692 3838; E-mail: feng@cs.su.oz.au.

0169-2607/94/$07.00
SSDI 0169-2607(94)01525-K

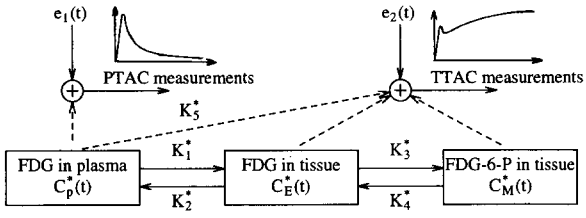

Fig. 1. A compartmental model used to describe the behavior of FDG in brain tissue. These three compartments represent, from left, vascular space for FDG, tissue space for free FDG and tissue space for FDG 6-phosphate. $K_1^* - K_4^*$ represent model transport rate constants and K_5^* is the vascular space fraction. $e_1(t)$, $e_2(t)$ are independent measurement noise at input and output, respectively. PTAC is the plasma time-activity curve and TTAC is the tissue time-activity curve.

TTAC as the model input and output functions, respectively [1]). Great attention has been paid in the last 2 decades to improving the parameter estimation accuracy with PET, by exploring model dependency [3], TTAC sampling schemes [4], parameter sensitivities [5], and estimation algorithms [6,7] etc., on the estimated values. Nevertheless, little attention has been paid to the effects of PTAC sampling schemes and errors on the accuracy of parameter estimation. Empirical PTAC sampling schedules are often used. The parameter estimation normally ignores PTAC errors and simply uses piecewise linear approximation of the measurement data as the model input directly. In some cases, however, the use of such input functions in modeling leads to statistical uncertainties in the estimated parameters, while careful design of proper PTAC sampling schedule and taking the PTAC measurement noise into account can improve the estimation quality. Recently, some researchers have started investigating the effects of input function measurement noise in tracer kinetic modeling with PET [8,9], but no detailed report so far has been found in the study of PTAC sampling schedule. The general purpose of this research is to study the effects of PTAC sampling schedule in tracer kinetic modeling with PET.

Measurements, especially in biomedical systems, are often scarce and far from noise-free, so the quality of biomedical system modeling and physiological parameter estimation depends heavily on the choice of measurement schedule. Therefore, optimal sampling schedule (OSS) for the model output function has been widely used to design experiments, based on the optimization of a suitable criterion, so as to return the maximum information from the experiments and to produce the most effective results in parameter estimation [10–20]. The most significant result of output function OSS achieved so far is that for a wide class of useful kinetic models, the maximum number of sampling times required in the subsequent parameter estimation for the maximum accuracy equals the minimum number required by algebraic constraints, which is also equal to the number of unknown and uniquely identifiable parameters [12,14]. This result greatly simplifies certain biomedical experiments where blood samples are required to be taken, as well as maximizes the information obtained from the experiments.

As in most of the studies, the input functions of the models are assumed to be known and require no measurements and hence require no sampling schedules. However, in tracer kinetic modeling with PET, the input functions are usually measured by taking blood samples. To study the input function optimal sampling schedule, a suitable model to describe the input tracer curve in blood is necessary. We recently proposed a PTAC model [21] to describe the complex FDG tracer kinetics in blood vessels. The study shows that this PTAC model can best fit the experimental data among many alternatives. In this paper, we particularly use this model to explore the optimal blood sampling schedule (OBSS) for the input functions and the effects of PTAC sampling schedules on the estimation accuracy and reliability of FDG model macro- and micro-parameters and physiological parameter local cerebral metabolic rates of glucose (LCMRGlc or R_i).

2. Methods

2.1. The PTAC model

The FDG tracer behavior in the circulatory system can be approximated by a model described in [21]. This model was represented by a 4th-order exponential curve with a pure delay and a pair of

repeated eigenvalues. To focus our attention on the effect of OBSS on LCMRGlc estimates in our later simulation study, we ignored the time delay term, as it does not affect the results of the present study. The model without delay term is:

$$C^*_P(t) = (A_1 t - A_2 - A_3)\, e^{\lambda_1(t)} + A_2\, e^{\lambda_2(t)} + A_3\, e^{\lambda_3(t)} \quad (2\text{-}1)$$

where * indicates decay-corrected FDG tracer quantities; λ_1, λ_2 and λ_3 (in l/min) are the eigenvalues of the system; A_1, A_2 and A_3 (in μCi/ml) are the coefficients. The original model (with delay term) was used to fit a typical set of experimental plasma time-activity data. If we delete the fitted delay parameter (a positive real number) from the fitted function, the simplified fitted function is:

$$\begin{aligned} C^*_P(t) = {} & (851.1225t - 20.8113 \\ & - 21.87981)\, e^{-4.133859t} \\ & + 20.8113\, e^{-0.01043449t} \\ & + 21.87981\, e^{-0.1190996t} \end{aligned} \quad (2\text{-}2)$$

This function has been used to improve the parameter estimation accuracy from noisy data [21] and to construct PTAC from the spillover contaminated left ventricular measurements in dynamic cardiac PET FEG studies [22]. In this paper, we use this function to derive the PTAC optimal sampling protocols.

2.2. OSS theory

Consider a single input/single output (SISO) dynamic system on the observation interval $[t_0, T]$ as follows [12,14]:

$$\mathrm{d}\mathbf{x}(t,\mathbf{p})/\mathrm{d}t = \mathbf{f}[\mathbf{x}(t,\mathbf{p}),\, u(t);\mathbf{p}] \quad (2\text{-}3)$$

$$\mathbf{x}(t_0,\mathbf{p}) = \mathbf{x}_0$$

$$y(t,\mathbf{p}) = \mathbf{g}[\mathbf{x}(t,\mathbf{p});\mathbf{p}] \quad (2\text{-}4)$$

$$z(t_k) = y(t_k,\mathbf{p}) + e(t_k) \quad (2\text{-}5)$$

$$k = 1,2, \ldots, N$$

where $\mathbf{x}$ is the n dimensional state vector; u and y are the scalar input and output, respectively; $\mathbf{f}$ and $\mathbf{g}$ are the linear or nonlinear functions which describe the structure of the system and output configurations, parameterized by the p-dimensional parameter vector $\mathbf{p}$; z is the measurement scalar, sampled at discrete times t_k; e is the measurement error, assumed to be white and zero mean with known variance $\sigma^2(t_k)$. We assume that the parameters are identifiable [2]. The measure for parameter information in data is the Fisher information matrix M, the inverse of which is a computable measure of the smallest variance-covariance matrix of the parameter estimation, $cov(\hat{p})$, i.e., the optimization is based on the Cramer-Rao theorem:

$$cov(\hat{p}) \geq M^{-1} \quad (2\text{-}6)$$

where $\hat{p}$ is the estimated parameter vector, $cov(\hat{p})$ is the variance-covariance matrix of the estimated parameters and M, M^{-1} are the Fisher information matrix and inverse matrix, respectively.

The theorem indicates that the smallest variance-covariance matrix of the estimates $cov(\hat{p})$ is M^{-1}. Therefore, the purpose of OSS is to minimize M^{-1} or maximize M. The solution used in practice, D-optimal, provides minimization of det (M^{-1}), where det (M^{-1}) is the determinant of M^{-1}, which is equivalent to maximizing det (M). Thus, to determine optimal sampling schedules, $t^*_1, t^*_2, \ldots, t^*_N$, the schedule $t_1, t_2, \ldots, t_N$ is algorithmically adjusted until det (M) is maximized. The element of M is:

$$m_{ij}(t_1, \ldots, t_n) = \sum_{k=1}^{n} \frac{1}{\sigma^2(t_k)} \left[\frac{\partial y(t_k,p)}{\partial p_i}\right] \left[\frac{\partial y(t_k,p)}{\partial p_j}\right] \quad (2\text{-}7)$$

The terms in brackets are the sensitivities of the output y with respect to the parameters p_i and p_j. This means that the optimization problem is generally nonlinear and optimum designs are therefore usually obtainable numerically, i.e., they

can be obtained as a result of a sequence of iterations and the procedure is repeated until the sampling schedules cease to change significantly within a prescribed tolerance.

We used the optimal sampling method described above to design the blood sampling schedules for the PTAC model of Eq. (2-2) and then applied the resultant sampling scheme to the following FDG model to estimate the transport rate constants and LCMRGlc.

2.3. The FDG model

The FDG model we use to estimate LCMRGlc consists of three compartments (see Fig. 1) which represents FDG concentration in plasma $C_P^*(t)$, FDG concentration in tissue $C_E^*(t)$, and FDG-6-P concentration in tissue $C_M^*(t)$, respectively. Details of this FDG model can be found in [4,23,24]. Usually, FDG concentration in plasma are measured by the samples of arterial or arterialized venous blood, while the ^{18}F concentration in tissue is scanned by PET. In this study, tissue concentration in the FDG model is expressed as follows:

$$C_t^*(t) = C_E^*(t) + C_M^*(t) + K_5^* C_P^*(t) \qquad (2\text{-}8)$$

$$= (B_1 e^{-L_1 t} + B_2 e^{-L_2 t}) \otimes C_P^*(t) + K_5^* C_P^*(t)$$

where $C_t^*(t)$ denotes the total ^{18}F activity in tissue, $\otimes$ is the convolution integration operator. B_1, B_2, L_1 and L_2 are the model impulse response function parameters (macroparameters); K_5^* is the vascular space fraction, has the unit ml/(g × min). B_1 and B_2 have the units ml/(g × min), L_1 and L_2 have the units l/min. And,

$$K_1^* = B_1 + B_2 \qquad (2\text{-}9)$$

$$K_2^* = \frac{B_1 L_1 + B_2 L_2}{B_1 + B_2} \qquad (2\text{-}10)$$

$$K_3^* = \frac{B_1 L_2 + B_2 L_1}{B_1 + B_2} - \frac{L_1 L_2 (B_1 + B_2)}{B_1 L_1 + B_2 L_2} \qquad (2\text{-}11)$$

$$K_4^* = \frac{L_1 L_2 (B_1 + B_2)}{B_1 L_1 + B_2 L_2} \qquad (2\text{-}12)$$

where $K_1^* - K_4^*$ are the FDG transport rate constants (microparameters). K_1^* has the unit ml/(g × min), $K_2^* - K_4^*$ have the units l/min.

The local cerebral metabolic rate of glucose R_i in the region of interest can be evaluated as follows:

$$R_i = \frac{1}{LC} \frac{K_1^* K_3^*}{K_2^* + K_3^*} C_P \qquad (2\text{-}13)$$

where LC is the lumped constant, knowledge of which represents the difference in terms of the transport kinetics between FDG and glucose, and C_p denotes the 'cold' glucose concentration in plasma. Further details and assumptions about LC can be found in [23]. In this paper, we use the same LC and 'cold' C_p values as in [23]. R_i has the unit mg/(100g × min).

In this paper, Eq. (2-2) is used as an input generator and the primary function to produce OBSS. Eq. (2-1) is utilized to fit PTAC based on the OBSS or conventional sampling schedule. Eq. (2-8) is then applied to estimate macroparameters B_1, B_2, L_1, L_2 and K_5^* and, finally, $K_1^* - K_4^*$ and LCMRGlc can be calculated from Eqs. (2-9)–(2-13).

3. Computer simulation

The first simulation was to optimize one currently used plasma sampling schedule, whose initial sampling schedule consisted of 19 time points generated at shorter intervals at the beginning of the study and at gradually longer intervals thereafter, for our PTAC function without delay term. A 5% blood sample noise CV (coefficient variance) was evenly used in all the samples. The optimization was done by a modified relaxing optimization program based on the OSS1 package from the Biocybernetics Laboratory at UCLA.

From the first simulation, we obtained one set of optimal blood sampling time points for our 6-parameter PTAC function. The resultant OBSS has basically 6 time points, constituting in total of 19 samples. Applying this new schedule in which 19 samples are distributed among these 6 time points and the traditional schedule in which 19 samples are distributed separately in 19 different points, we performed the second set of simulations

to estimate LCMRGlc and then compared the effects of the OBSS and non-OBSS on the accuracy and reliability of LCMRGlc estimates.

The FDG model rate constants we used here were a set of average parameters in grey matter calculated from 13 normal volunteers according to [23] ($K_1^* = 0.102$ ml/(g × min), $K_2^* = 0.130$ min^{-1}, $K_3^* = 0.0068$ min^{-1}, $K_4^* = 0.0334$ min^{-1}, $C_p = 91.9$ mg/100ml, $LC = 0.418$) and vascular space fraction $K_5^* = 0.05$ ml/(g × min). The following output scanning sequence was used: 10 × 12-s scans, 2 × 0.5-s scans, 2 × 1-min scans, 1 × 1.5-min scan, 1 × 3.5-min scan, 2 × 5-min scans, 1 × 10-min scan and 3 × 30-min scans.

In the second set of the simulation, we assumed that the measurements of plasma and total FDG activity in tissue are $x(t)$ and $y(t)$, respectively, and the measurement noise e_1 and e_2 in $x(t)$ and $y(t)$ are independent Gaussian distributions with zero mean. Thus,

$$x(t_i) = C_p^*(t_i) + e_1(t_i) \text{ and}$$

$$y(t'_j) = C_t^*(t'_j) + e_2(t'_j) \tag{3-1}$$

In PET studies, the variance of measurement noise e_i ($i = 1,2$) can have different forms, depending on the way the data are collected. Since the tracer blood activity is obtained directly from the blood samples, c_1, the coefficient of variation of PTAC measurements, can be assumed to be constant at different sampling times as described below:

$$Var(e_1(t_i)) = (c_1 \times C_p^*(t_i))^2 \tag{3-2}$$

where $Var(e_1(t_i))$ is the variance of PTAC measurement noise e_1 at time t_i.

On the other hand, since $y(t'_j)$ is actually the average of total count during the scan period in the practical PET studies, the TTAC measurement noise variance is proportional to the radioactivity concentration and inversely proportional to the length of the scan interval, which can be described as follows:

$$Var(e_2(t'_j)) = \frac{c_2 \times C_t^*(t'_j)}{\Delta t'_j} \tag{3-3}$$

where $Var(e_2(t'_j))$ is the variance of TTAC measurement noise e_2 at time t'_j, c_2 is the coefficient of variation of TTAC measurements and $\Delta t'_j = t'_j - t'_{j-1}$ is the scan interval at time t'_j.

Then, we used Eq. (3-2), Eq. (3-3) to generate pseudo-noise series $e_1(t_i)$ and $e_2(t'_j)$ for PTAC and TTAC measurement data, respectively. In order to focus on the effect of PTAC sampling schedule on the accuracy of LCMRGlc estimates we varied c_1 at 0, 2.5, 5, 10, 15 and 20%, forming 6 PTAC noise levels while fixing c_2 to 0.5, equivalent to 2% of deviation at the last point of TTAC measurements.

In the weighted least-square nonlinear regression, the weights should be inversely proportional to the noise variance. Therefore, the weight we used in our PTAC function estimation was:

$$w(C_p^*(t_i)) = \frac{1}{(c_1 \times C_p^*(t_i))^2} \tag{3-4}$$

where $w(C_p^*(t_i))$ is the weight factor at time t_i in the PTAC function estimation. Similarly, the weight in the FDG model macroparameter estimation was:

$$w(C_t^*(t'_j)) = \frac{1}{\frac{c_2 \times C_t'(t'_j)}{\Delta t'_j}} \tag{3-5}$$

where $w(C_t^*(t'_j))$ is the weight factor at time t'_j in the FDG model macroparameter estimation.

Three methods have been used: (a) estimating the FDG model macroparameters ignoring PTAC noise. This method, which is currently used in tracer kinetic modeling with PET where PTAC measurement is assumed noise-free, has nothing to do with OBSS since there is no analytical input function. The second and third methods took PTAC noise into account by estimating the PTAC parameters based on the generated OBSS and currently used sampling protocols: (b) estimating the PTAC and the FDG model macroparameters simultaneously, (c) estimating the PTAC model parameters first, then the FDG model macroparameters. Various statistical values, such as mean, bias and standard deviation, were calculated from 100 simulations for all three methods, using BLD — a software system for physiological data handling and model analysis [25].

4. Results and discussion

The results of the first simulation concerning OBSS for the PTAC function was summarized in Table 1. In the table, the initial sampling schedule which was carefully chosen during practical experiments without using normal optimization is listed first and then the sample boundaries are given. The final OBSS includes basically 6 time points at about 0.05, 0.683, 2.025, 12.85, 46.38, 145 min. The samples are replicated at these 6 time points. From the last row of the table, we can see the estimated parameter CV reduced in OBSS, which is partially due to the optimization of the sampling schedule and partially due to the introduction of the 0.05 min as the lower bound of the sampling schedule. Furthermore, samples are only taken from 6 different points in OBSS which greatly simplifies the operation of taking blood samples during the experiments.

Please note that the sampling time corresponding to the PTAC peak value is not included in OBSS. In other words, with the application of the PTAC model and OBSS, the peak sampling time is not critical as the peak value can be predicated from the fitted PTAC curve rather than directly measured, as previously required.

The second group of simulation is for evaluating the effects of PTAC measurement noise on the accuracy of LCMRGlc estimates based on both the non-OBSS and OBSS measurements. The time points of OBSS and non-OBSS (initial schedule) are shown in Table 1. According to DiStefano [14], the additional samples should be distributed at the same optimal times in a minimum size schedule, not in between, and each point in a minimum size optimal schedule of time points determined by maximizing det (M), carrying the same weight in its contribution to overall accuracy. Therefore, samples consisting of replicates at the same 6 optimal sampling points should provide maximum accuracy [12,14]. Tables 2–4 illustrate the results of this set of simulations using methods (a), (b), and (c) mentioned above when PTAC noise level is 5, 10, and 20%, respectively.

In these tables, the nominal values, i.e., the true values for the FDG model's macroparameters, microparameters and LCMRGlc are given first. Then the means, biases and standard deviations of the estimates from 100 simulations using method (a), which ignores PTAC noise are provided. And then the same statistical values are listed for method (b), which takes PTAC measurement noise into account and estimates all the input and the FDG model macroparameters simultaneously, based on OBSS and non-OBSS, respectively. At last all these values are given for method (c), which also takes PTAC measurement noise into account, but estimates the input parameters first and then the FDG model macroparameters based on OBSS and non-OBSS, respectively.

Table 2 illustrates the estimated results when the

Table 1
Nineteen blood sample schedule for the 6-parameter PTAC function

Number of samples	19
Initial schedule	0.79 0.94 1.13 1.31 1.49 1.69 1.87 2.04 2.59 3.33 4.64 7.13 10.03 15 20 30.61 61.15 90 145
Sample boundary	0.05–145 min
Constant CV	5% (for all examples)
Optimal schedule	(0.05 0.05 0.05) (0.683 0.683 0.683 0.683) (2.025 2.025 2.025 2.025) (12.85 12.85 12.85 12.85) (46.38 46.38) (145.0 145.0)

Nominal para values	Optimized para CV (%)	Initial para CV (%) (paren values if samples are duplicated)
$A1 = 851.1225$	3.61 (2.55)	58.11 (41.09)
$\lambda_1 = -4.13386$	2.99 (2.11)	17.83 (12.61)
$A2 = 20.81130$	5.16 (3.65)	6.90 (4.88)
$\lambda_2 = -0.01043$	4.76 (3.37)	6.69 (4.73)
$A3 = 21.87981$	7.92 (5.60)	8.44 (5.97)
$\lambda_3 = -0.11910$	14.61 (10.33)	19.54 (13.82)

Table 2
Comparison of parameter estimates of ignoring and taking PTAC measurement noise into account when the 5% PTAC noise is added

		Macroparameters					Rate constants				LCMRGlc
		B_1	L_1	B_2	L_2	K_5*	K_1*	K_2*	K_3*	K_4*	R_i
P		**0.034547**	**0.004551**	**0.067453**	**0.194249**	**0.05**	**0.102**	**0.13**	**0.062**	**0.0068**	**7.241522**
(a) Ignore	Mean	0.03336	0.004305	0.07037	0.19704	0.05047	0.10373	0.13593	0.05896	0.00646	6.9906
PTAC	Bias (%)	3.6	5.8	4.1	1.4	0.9	1.6	4.3	5.1	5.3	3.6
Noise	S.D.	0.0038	0.0015	0.0223	0.0839	0.0248	0.0236	0.0673	0.0195	0.0024	0.7628
(b) Simu.	Mean	0.03373	0.004243	0.06933	0.19424	0.05050	0.10305	0.13289	0.05916	0.00642	7.0648
Estim.	Bias (%)	2.4	7.3	2.7	0.01	1.6	0.97	2.2	4.7	5.9	2.5
Non-OBSS	S.D.	0.0033	0.0012	0.0212	0.0763	0.0250	0.0220	0.0616	0.0178	0.0021	0.6660
(b) Simu.	Mean	0.03458	0.004529	0.07442	0.22172	0.04378	0.10900	0.15441	0.06507	0.00677	7.2570
Estim.	Bias (%)	0.1	0.5	9.4	12	14	6.4	16	4.8	0.4	0.2
OBSS	S.D.	0.0029	0.0011	0.0261	0.1049	0.0243	0.0271	0.0883	0.0203	0.0018	0.6312
(c) Sepa.	Mean	0.03373	0.004241	0.06926	0.19400	0.04923	0.10299	0.13269	0.05913	0.00642	7.0648
Estim.	Bias (%)	2.4	7.3	2.6	0.12	1.5	0.96	2.0	4.9	5.9	2.5
Non-OBSS	S.D.	0.0033	0.0012	0.0212	0.0758	0.0250	0.0220	0.0613	0.0177	0.0021	0.6626
(c) Sepa.	Mean	0.03458	0.004527	0.07432	0.22136	0.04381	0.10890	0.15402	0.06510	0.00677	7.2577
Estim.	Bias (%)	0.1	0.5	9.3	12	14	6.3	15.6	4.8	0.43	0.2
OBSS	S.D.	0.0029	0.0011	0.0258	0.1029	0.0243	0.0267	0.0864	0.0202	0.0018	0.6298

Table 3
Comparison of parameter estimates of ignoring and taking PTAC measurement noise into account when the 10% PTAC noise is added

		Macroparameters					Rate constants				LCMRGlc
		B_1	L_1	B_2	L_2	K_5*	K_1*	K_2*	K_3*	K_4*	R_i
P		**0.034547**	**0.004551**	**0.067453**	**0.194249**	**0.05**	**0.102**	**0.13**	**0.062**	**0.0068**	**7.241522**
(a) Ignore	Mean	0.03317	0.004157	0.07414	0.22327	0.05411	0.10732	0.15698	0.06420	0.00625	6.9870
PTAC	Bias (%)	4.2	9.4	9.0	13.0	7.6	4.9	17	3.4	8.8	3.6
Noise	S.D.	0.0054	0.0021	0.0270	0.1442	0.0277	0.0289	0.1152	0.0327	0.0033	1.0569
(b) Simu.	Mean	0.03362	0.004160	0.07474	0.22508	0.05190	0.10836	0.15864	0.06439	0.00621	7.0765
Estim.	Bias (%)	2.8	9.4	9.8	13.7	3.7	5.8	18.0	3.7	9.5	2.3
Non-OBSS	S.D.	0.0045	0.0016	0.0285	0.1454	0.0277	0.0302	0.1182	0.0306	0.0025	0.9286
(b) Simu.	Mean	0.03403	0.004284	0.078042	0.22650	0.04749	0.11207	0.16104	0.06343	0.0063	7.1662
Estim.	Bias (%)	1.5	6.3	13.6	14.2	5.3	9.0	19.2	2.2	7.6	1.1
OBSS	S.D.	0.0038	0.0013	0.0213	0.0892	0.0276	0.0221	0.0682	0.0252	0.0021	0.8015
(c) Sepa.	Mean	0.03361	0.004140	0.07443	0.22380	0.05205	0.10803	0.15748	0.06428	0.00618	7.0727
Estim.	Bias (%)	2.8	9.9	9.4	13.2	3.8	5.6	17.5	3.6	10.0	2.4
Non-OBSS	S.D.	0.0044	0.0016	0.0276	0.1404	0.0272	0.0292	0.1134	0.0301	0.0025	0.8997
(c) Sepa.	Mean	0.03403	0.004282	0.077722	0.22538	0.04759	0.11175	0.15992	0.06342	0.00632	7.1660
Estim.	Bias (%)	1.5	6.3	13.3	13.8	5.0	8.7	18.7	2.2	7.6	1.1
OBSS	S.D.	0.0037	0.0012	0.0210	0.0843	0.0459	0.0216	0.0648	0.0241	0.0021	0.7791

Table 4
Comparison of parameter estimates of ignoring and taking PTAC measurement noise into account when the 20% PTAC noise is added

		Macroparameters					Rate constants				LCMRGlc
		B_1	L_1	B_2	L_2	K_5*	K_1*	K_2*	K_3*	K_4*	R_i
P		**0.034547**	**0.004551**	**0.067453**	**0.194249**	**0.05**	**0.102**	**0.13**	**0.062**	**0.0068**	**7.241522**
(a) Ignore	Mean	0.03253	0.003859	0.07646	0.22920	0.04950	0.10898	0.16360	0.06369	0.0057	6.8867
PTAC	Bias (%)	6.1	17.9	11.8	15.2	1.0	6.4	20.5	2.7	17.3	5.2
Noise	S.D.	0.0079	0.0030	0.0299	0.2050	0.0302	0.0338	0.1685	0.0418	0.0045	1.5475
(b) Simu.	Mean	0.03304	0.003872	0.07649	0.21514	0.04814	0.10953	0.15277	0.06050	0.00574	6.9592
Estim.	Bias (%)	4.5	17.6	11.8	9.7	3.7	6.8	14.9	2.5	19.2	4.1
Non-OBSS	S.D.	0.0058	0.0020	0.0273	0.1375	0.0310	0.0297	0.1084	0.0320	0.0031	1.1673
(b) Simu.	Mean	0.03355	0.004188	0.082793	0.25305	0.04336	0.11634	0.18424	0.06679	0.00621	7.0902
Estim.	Bias (%)	3.0	8.6	18.5	23.2	15.2	12.3	29.4	7.2	9.3	2.1
OBSS	S.D.	0.0060	0.0023	0.0228	0.1190	0.0235	0.0251	0.0908	0.0319	0.0035	1.1608
(c) Sepa.	Mean	0.03274	0.003706	0.07655	0.21488	0.04827	0.10929	0.15288	0.06024	0.00546	6.9116
Estim.	Bias (%)	5.5	22.7	11.9	9.6	3.5	6.7	15.0	2.8	23.8	4.8
Non-OBSS	S.D.	0.0059	0.0020	0.0260	0.1379	0.0309	0.0285	0.1077	0.0326	0.0031	1.1912
(c) Sepa.	Mean	0.03376	0.004117	0.078231	0.23677	0.04867	0.11199	0.16818	0.06649	0.00622	7.1150
Estim.	Bias (%)	2.3	10.4	13.8	17.9	2.7	8.9	22.7	6.8	9.3	1.8
OBSS	S.D.	0.0055	0.0021	0.0396	0.1791	0.0338	0.0417	0.1490	0.0385	0.0033	1.1175

5% PTAC noise level was used. In this table, when PTAC measurement noise is taken into consideration based on non-OBSS as well as OBSS, the mean of LCMRGlc is improved by about 30 and 94% respectively; and 13 and 17% improvement for S.D. are achieved, respectively using method (b) versus method (a). Similar improvements are achieved by using method (c) versus method (a). From these results, we can see that the mean improvements using OBSS are very large in comparison to non-OBSS. All other statistical values, which are more important in parameter estimation, are also better using both method (b) and method (c).

In Table 3 where the 10% PTAC noise was used, the mean of LCMRGlc is improved by about 35 and 70%, respectively and 12 and 24% improvement for S.D. are achieved, based on non-OBSS and OBSS, respectively using method (b) versus method (a). Again, similar improvements are achieved when used method (c) versus method (a).

In Table 4 where the 20% PTAC noise was used, the mean of LCMRGlc is improved by about 20 and 57%, respectively; and 24 and 25% improvements for S.D. are achieved based on non-OBSS and OBSS, respectively using method (b) versus method (a). At this noise level the mean is improved by 7 and 64%, respectively while S.D. is improved by 23 and 28% based on non-OBSS and OBSS, respectively using method (c) versus method (a).

From Tables 2–4, it is clear that taking PTAC noise into account can provide more accurate and reliable estimates of LCMRGlc, particularly for those using OBSS. Although within methods (b) and (c) some of the individual model parameter estimates based on OBSS are not as good as those based on non-OBSS, the physiological parameter LCMRGlc, which is the combination of all of the individual estimates, is significantly improved if OBSS is used.

Fig. 2 illustrates the LCMRGlc mean improvements (compared with ignoring PTAC measurement noise) when account is taken of PTAC measurement noise as a function of PTAC noise levels, using OBSS and non-OBSS. The two sets of curves in the diagram represent the improvements of the estimate bias using methods (b) and (c) versus (a). The average improvements of these two methods are all about 71% using OBSS and 28% using non-OBSS. The way to calculate these improvements is:

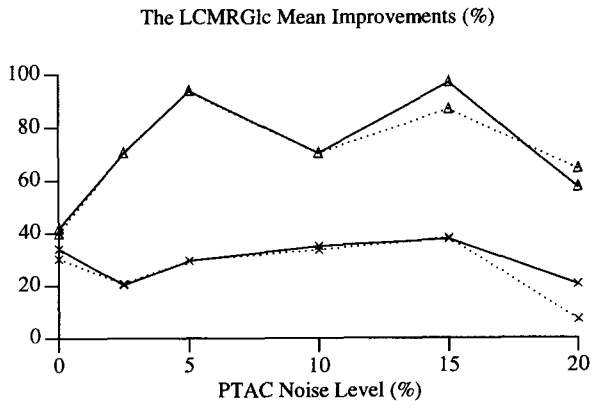

Fig. 2. Plots of the LCMRGlc mean improvements versus PTAC noise level when PTAC measurement noise is accounted for, based on both OBSS and non-OBSS. Estimate input and the FDG model macroparameters using: simultaneously OBSS (——Δ——), separately OBSS (· · Δ · ·), simultaneously non-OBSS (—— × ——) and separately non-OBSS (· · × · ·)

$$\left\{1 - \frac{\Delta P \text{ of method (b) or (c)}}{\Delta P \text{ of method (a)}}\right\} \times 100\% \quad (4\text{-}1)$$

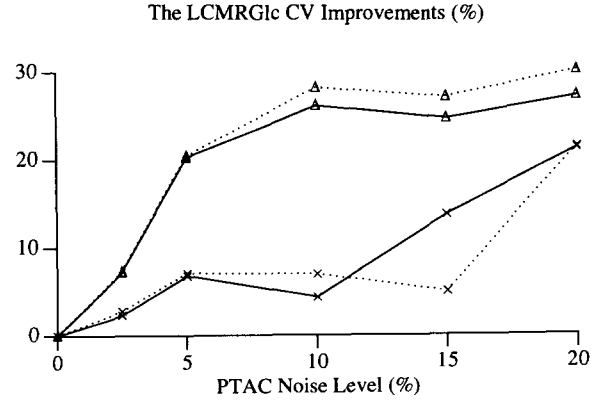

Fig. 3. Plots of the LCMRGlc CV improvements versus PTAC noise level when PTAC measurement noise is accounted for, based on both OBSS and non-OBSS. Estimate input and the FDG model macroparameters using: simultaneously OBSS (——Δ——), separately OBSS (· · Δ · ·), simultaneously non-OBSS (—— × ——) and separately non-OBSS (· · × · ·).

Plots of the relative improvements of CV of LCMRGlc when the input measurement noise was accounted for, using OBSS and non-OBSS are illustrated in Fig. 3. In the diagram these four curves represent the improvements of CV using method (b) and (c) versus (a). Using OBSS, the average improvements of these two methods are all about 20% while the average improvements of these 2 methods are all about 12% using non-OBSS. The equation to calculate these improvements is:

$$\left\{1 - \frac{\text{CV of method (b) or (c)}}{\text{CV of method (a)}}\right\} \times 100\% \quad (4\text{-}2)$$

When we set $c_1 = 0$, there was no PTAC noise added in the simulation. These results focus on the effects of different operations of convolution used on LCMRGlc estimates. In method (a) where there was no explicit input function, only numerical convolution could be used. On the other hand, mathematical convolution has been used in method (b) and (c) where the proposed input function made the accurate convolution possible no matter which PTAC sampling schedule was used. It is reasonable that there is no improvement in the LCMRGlc S.D., though there is a bit of improvement in the LCMRGlc mean, which is mainly due to the use of the mathematical convolution, as shown in Figs. 2 and 3. From Tables 2–4 and Figs. 2 and 3, we can see that significant improvements in LCMRGlc estimation accuracies (S.D.) are achieved using OBSS, especially when PTAC noise is increased, compared with those determined from the initial 19 time point schedule.

All the results obtained here show that sampling schedule optimization is an effective approach to maximizing FDG model parameters and the physiological parameter estimation accuracies. Therefore, the application of OBSS in tracer kinetic modeling with PET can improve the quality of model and physiological parameter estimation, as well as simplifying the experiment operations for taking blood samples.

References

[1] S.C. Huang, R.E. Carson and M.E. Phelps, Tracer kinetic modeling in positron emission tomography, in: Tracer Kinetics and Physiologic Modeling, R.M. Lambrecht and A. Rescigmo, Eds., pp. 298–344, (Springer-Verlag, New York, 1983).

[2] E.R. Carson, C. Cobelli and L. Finkelstein, The Mathematical Modeling of Metabolic and Endocrine Systems, (John Wiley & Son, New York, 1983).

[3] S.C. Huang, D. Feng and M.E. Phelps, Model dependency and estimation reliability in measurement of cerebral oxygen utilization rate with oxygen-15 and dynamic positron emission tomography, J. Cereb. Blood Flow Metab. 6 (1986) 105–119.

[4] R.A. Hawkins, M.E. Phelps and S.C. Huang, Effects of temporal sampling, glucose metabolic rates, and disruptions of the blood-brain barrier on the FDG model with and without a vascular compartment: studies in human brain tumors with PET, J. Cereb. Blood Flow Metab. 6 (1986) 170–183.

[5] S.C. Huang, M.E. Phelps, E.J. Hoffman and D.E. Kuhl, Error sensitivity analysis of fluorodeoxyglucose method for measurement of cerebral metabolic rate of glucose, J. Cereb. Blood Flow Metab. 1 (1981) 391–401.

[6] D. Feng and D. Ho, Parametric imaging algorithms for multi-compartmental model dynamic studies with positron emission tomography, Ann. Nucl. Med. 7 (1993) S33.

[7] D. Feng, Z. Wang and S.C. Huang, A study on statistically reliable and computationally efficient algorithms for the measurement of local cerebral blood flow with positron emission tomography, IEEE Trans. Med. Imaging 12(2) (1993) 182–188.

[8] K. Chen, S.C. Huang and D.C. Yu, The effects of measurement errors in plasma radioactivity curve on parameter estimation in positron emission tomography, Phys. Med. Biol. 36(9) (1991) 1183–1200.

[9] R.H. Huesman and B.M. Mazoyer, Kinetic data analysis with a noisy input function, Phys. Med. Biol. 32(12) (1987) 1569–1579.

[10] C. Cobelli and A. Ruggeri, Optimal design of sampling schedules for studying glucose kinetics with tracers, Am. J. Physiol. 257 (1989) E444–E450.

[11] C. Cobelli and A. Ruggeri, A reduced sampling schedule for estimating the parameters of the glucose minimal model from a labeled IVGTT, IEEE Trans. Biomed. Eng. 38(10) (1991) 1032–1039.

[12] C. Cobelli, A. Ruggeri, J.J. DiStefano III and E.M. Landaw, Optimal design of multioutput sampling schedules — software and applications to endocrine — metabolic and pharmacokinetic models, IEEE Trans. Biomed. Eng. 32(4) (1985) 249–256.

[13] D.Z. D'Argenio, Optimal sampling times for pharmacokinetic experiments, J. Pharmacokin. Biopharm. 9(6) (1981) 739–756.

[14] J.J. DiStefano III, Optimized blood sampling protocols and sequential design of kinetic experiments, Am. J. Physiol. (1981) R259–R265.

[15] J.J. DiStefano III, Biomodel Formulation and Identification Using Optimal and Other Effective Experiment Design, Proc. IFAC Modeling and Control in Biomedical Systems, pp. 1–12, (Venice, Italy, 1988).

[16] J.J. DiStefano III, M. Jang, T.K. Malone and M. Broutman, Comprehensive kinetics of triiodothyronine production, distribution, and metabolism in blood and tissue pools of the rat using optimized blood-sampling protocols, Endocrinology 110(1) (1982) P198–P213.

[17] G.C. Goodwin and R.L. Payne, Choice of sampling intervals, in: System Identification: Advances and Case Studies, (Academic, New York, 1976).

[18] F. Mori and J.J. DiStefano III, Optimal nonuniform sampling interval and test input design for identification of physiological systems from very limited data, IEEE Trans. Automatic Control AC-24(6) (1979).

[19] A. Ruggeri and C. Cobelli, Optimal Sampling Schedule Design May Reveal Inadequacy of Model Structure: A Case Study on the Minimal Model of Glucose Disappearance, Proc. IFAC Modeling and Control in Biomedical Systems, pp. 121–126, (Venice, Italy, 1988).

[20] E. Walter and L. Pronzato, Qualitative and quantitative experiment design for phenomenological models, Automatica 269(2) (1990) 195–213.

[21] D. Feng, S.C. Huang and X. Wang, Models for computer simulation studies of input functions for tracer kinetic modelling with positron emission tomography, Int. J. Biomed. Comput. 32 (1993) 95–110.

[22] D. Feng and X. Li, Constructing tracer plasma time-activity curve (PTAC) from the contaminated left ventricular measurements in dynamic cardiac PET FEG studies and improving the estimation of MMRGLc, J. Nucl. Med. 34(5) (1993) 185.

[23] S.C. Huang, M.E. Phelps, E.J. Hoffman, K. Sideris, C.J. Selin and D.E. Kuhl, Non-invasive determination of local cerebral metabolic rate of glucose in man, Am. J. Physiol. 238 (1980) E69–E82.

[24] K. Wienhard, G. Pawlik, K. Herholz, R. Wagner and W.D. Heiss, Estimation of local cerebral glucose utilization by positron emission tomography of (F-18)2-fluoro-2-deoxy-D-glucose: a critical appraisal of optimization procedure, J. Cereb. Blood Flow Metab. 5 (1985) 115–125.

[25] R.E. Carson, S.C. Huang and M.E. Phelps, BLD — a software system for physiological data handling and model analysis, Proc. 5th Annual Symposium on Computer Application in Medical Care, IEEE Comput. Soc. (1981) 562–565.